Earth`s Cryosphere, 2015, vol. XIX, No. 4, pp. 74–83 **http://earthcryosphere.ru/**

OPERATION OF TWO-PHASE THERMOSYPHONS WITH HORIZONTAL EVAPORATOR TUBES: CAUSES OF INSTABILITY

J.B. Gorelik

Earth Cryosphere Institute, SB RAS, P/O box 1230, Tyumen, 625000, Russia; gorelik@ikz.ru

The operation of refrigeration systems based on natural convection (two-phase thermosyphons), with horizontal evaporator tubes, has been tested in the field on full-size devices and in laboratory on models. Both filed and laboratory testing shows the lack of sustainability in thermosyphon operation. According to laboratory data, the problem is due to return flow inevitably arising in the coolant path along the tube and producing the slug and plug regime known in counter-flow two-phase systems. A method is suggested to improve the sustainability of thermosyphons. It is efficient in laboratory but may fail in the field, and further research is needed to find appropriate solutions.

Thermosyphon, condenser, evaporator, two-phase flow, hydraulic resistance, saturation temperature, heat transfer, cooling

INTRODUCTION

Two-phase cooling systems based on natural convection (thermosyphons), with horizontal evaporation tubes, allow using pad foundations instead of piling in some types of structures, which saves labor costs. *Fundamentstroiarkos* was the first Russian company employing such systems in construction engineering for permafrost stabilization [*Dolgikh et al., 2004; Dolgikh and Okunev, 2006; Velchev and Sizikov, 2008*].

Before coming into civil engineering, systems of this kind were employed in nuclear power and metal industries for cooling nuclear and blast furnaces, respectively [*Kutepov et al., 1986; Pioro et al., 1991*], where thermal loads on the cooling system elements were orders of magnitude greater than in soil heat exchange. Testing of such systems in permafrost conditions has very little literature. Two-phase thermosyphons with horizontal or inclined tubes, used mainly to speed up concrete aging, were reported long ago [*Lyakh et al., 1978*] to lack sustainability in operation, and those early results were confirmed by later studies [*Gorelik and Gorelik, 2011*]. The blockage of a laboratory system and the impeded fluid circulation in the evaporator were demonstrated in a video at TICOP [*Gorelik, 2012*].

It is very difficult to test full-size samples of thermosyphons used in construction engineering, with 500 m or longer tubes (~1:10 000 diameter/length ratio) and large condensation units. In this respect, monitoring results from specific objects can be useful, with detailed descriptions of measurements (data on soils, foundation design, climate, measurement network and instruments, time since the beginning of operation and monitoring, periodicity of measurements), as well as methods for discrimination between thremosyphon cooling and natural ground cooling in cold seasons. However, no such publications are available.

On the other hand, the existing theoretical approaches neglect important features of two-phase flow in evaporators at relatively small thermal loads and fail to predict the time when the operation of such a system in the field may be blocked (as it happens in laboratory).

HISTORIC BACKGROUND

A full-size thermosyphon model with horizontal evaporation was designed by *Dolgikh and Okunev* [*1989*] and their colleagues who reported testing results [*Feklistov et al., 2008; Pazderin and Gilev, 2011*] and described the design for thermal stabilization of permafrost [*Dolgikh et al., 2011*]. The system operation is maintained by closed natural convection of a two-phase working fluid (vapor + liquid): the liquid warms up by taking heat from soil and evaporates in a tube; the mixed fluid with continuously increasing vapor share moves along the tube toward a condensing unit, where the vapor gives up heat to air and condenses, and the condensed fluid gravitates back to the evaporator, together with some portion of the originally liquid phase. The system is designed as direct single-flow cooling, i.e., the condensed fluid flow and the return vapor flow follow different paths, unlike the counter-flow systems where both the down-going condensate and the returning up-going vapor move along the same path, and the counter flows interact, which increases the system's hydraulic resistance.

The system described by *Dolgikh and Okunev* [*1989*] is charged with an ammonia coolant and consists of a 120 to 800 m long evaporator tube, 32 mm in diameter, and a cylindrical condensation tank cooled by refrigerating machines; an electric heater mounted all along the tube causes thermal load on the evaporator. Heat flux from the heater per tube unit length varies from 10 to 40 W/m (or 100–400 W/m^2 for the

a

Date	Fluid	Tube length, m	Condenser height, m	Fluid level, mm	Air temperature, °C	Fluid temperature, °C	Mean wall temperature, °C	Specific heat, W/m	Mean vapor volume content
1	2	3	4	5	6	7	8	9	10
04.10.90	Ammonia	600	1.8	210	8.41	–10.5	–6.08	86.55	653.17

b

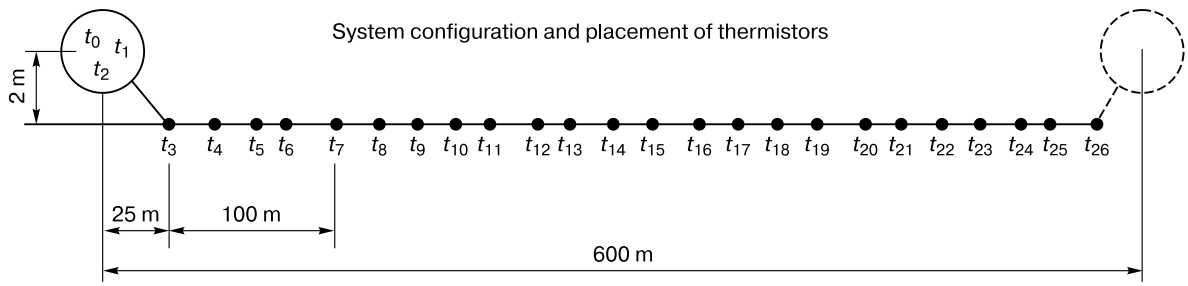

c

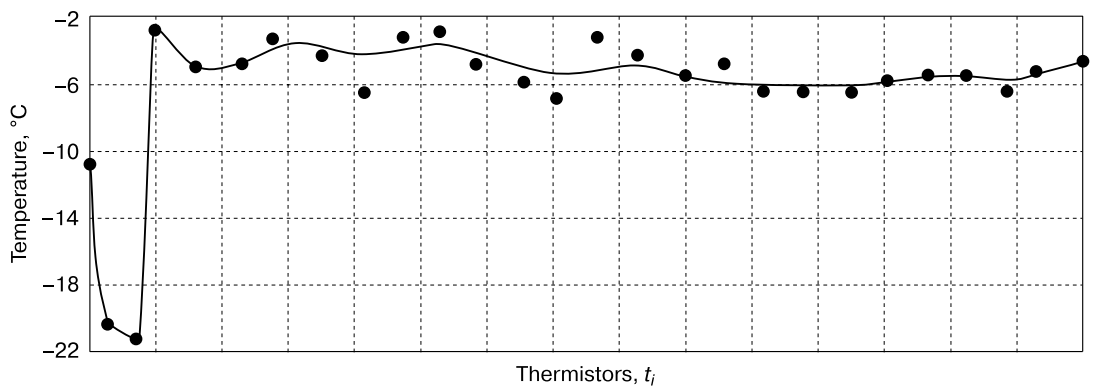

Fig. 1. Parameters of a model system and conditions of tests by *Dolgikh and Okunev* [*1989*].

a – testing conditions; *b* – position of condenser relative to evaporator (solid circle is condenser with evaporator outlet and dash circle is condenser with evaporator inlet, both circles correspond to the same object) and placement of thermistors (t_3 – t_{26}) on evaporator; *c* – temperature variations along evaporator (thermistors are at same points as in Fig. 1, *b*).

known tube diameter) being orders of magnitude lower than in large industrial systems but times higher than that from soil. Temperature variations along the tube show different patterns depending on the condenser height above the evaporator and on cooling conditions [*Dolgikh and Okunev, 1989*]. A test example is shown in Fig. 1 (data on curves presented by *Dolgikh and Okunev* [*1989*] are readings taken two hours after the system start).

Sustainable operation of the system providing free sinking of the condensate into the evaporator requires the sum $P_c + P_g$ (P_c is the saturation vapor pressure in the condenser and P_g is the hydrostatic pressure of the condensate rising above the evaporator) to exceed the pressure at the coolant boiling point in the evaporator (P_b):

$$\Delta P = P_c + P_g - P_b > 0, \quad (1)$$

while

$$P_g = \rho g H_c, \quad (2)$$

where ρ is the density of the coolant (ammonia); g is the gravity acceleration; H_c is the height difference between the condensate level in the condenser and the evaporator (the value 2 m in Fig. 1, *b* is the sum of 1.8 m and 0.21 m in columns 4 and 5 of Table in Fig. 1, *a*). The pressures P_c and P_b are found from temperature measurements at the respective condenser and evaporator points (Fig. 1, *b*, *c*) and the saturation curve for the given coolant. As laboratory tests show, temperatures vary markedly across the condenser surface (even at complete evaporation) due to variable heat exchange with the ambience and condensation patterns. Therefore, direct pressure measurements are recommended for exact

Table 1. **Pressure and pressure gradient within the segment of liquid flow in a model thermosyphon**

Test number	t_c, °C	P_c, bar	H_c, m	P_g, bar	t_b, °C	P_b, bar	ΔP
1	−3.75	3.85	2.00	0.13	−1.0	4.18	−0.20
2	−10.50	3.04	2.01	0.13	−2.2	4.04	−0.87
3	−4.25	3.79	3.185	0.20	−2.2	4.04	−0.05
4	−11.25	2.95	3.20	0.205	−6.0	3.58	−0.42
5	−2.25	4.03	3.185	0.20	0.1	4.31	−0.08
6	−3.75	3.85	3.21	0.206	−1.0	4.18	−0.12
7	−15.0	2.50	1.935	0.12	−11.0	2.98	−0.36
8	−5.0	3.70	3.150	0.202	−1.9	4.07	−0.15
9	−16.0	2.38	3.135	0.201	−10.0	3.10	−0.52
10	15.2	7.56	1.95	0.125	17.0	7.955	−0.27
11	−12.5	2.80	1.955	0.125	−8.0	3.34	−0.415
12	9.0	6.235	3.14	0.202	9.8	6.41	0.03
13	−10.5	3.04	3.15	0.202	−8.8	3.34	−0.10

Note. According to experiments of *Dolgikh and Okunev* [*1989*].

Table 2. **Pressure and pressure gradient within the segment of liquid flow in a full-size thermosyphon**

Test number	t_c, °C	P_c, bar	H_c, m	P_g, bar	t_b, °C	P_b, bar	ΔP
1	−8.4	3.29	2.71	0.17	−6.9	3.47	−0.01
2	−2.0	4.06	2.71	0.17	−0.2	4.27	−0.04
3	−1.6	4.12	2.71	0.17	−0.9	4.23	0.06
4	0.3	4.36	2.71	0.17	2.2	4.77	−0.24
5	−1.3	4.14	2.71	0.17	0.2	4.34	−0.03
6	−0.3	4.26	2.71	0.17	1.0	4.51	−0.08
7	−2.2	4.03	2.71	0.17	−1.0	4.22	−0.02
8	−1.6	4.12	2.71	0.17	−0.3	4.33	−0.04
9	−4.2	3.73	2.71	0.17	−2.9	3.92	−0.02
10	−6.8	3.48	2.71	0.17	−4.7	3.74	−0.09
11	−2.0	4.06	2.71	0.17	−0.2	4.28	−0.05
12	−3.5	3.83	2.71	0.17	−2.3	4.02	−0.02
13	−0.6	4.23	2.71	0.17	2.6	4.86	−0.46

Note. According to experiments of *Feklistov et al.* [*2008*].

estimation of P_c. The temperature t_c corresponding to the pressure P_c according to the saturation curve is given in column 7 of Table in Fig. 1, *a*, while the temperature t_b corresponds to the coolant boiling point at the evaporator inlet where the temperature rises dramatically at t_3 (Fig. 1, *c*).

Note that condition (1) fails in almost all tests except 12 (Table 1), where temperature data are of low quality. Thus, there is no circulation (unidirectional flow of two-phase fluid) required for cooling.

Similar experiments were run at a test site of the *Fundamentstroiarkos* company with tube lengths from 200 to 1000 m (Table 2) [*Feklistov et al., 2008*], in winter, when the condenser was naturally cooled by air. However, *Feklistov et al.* [*2008*] did not specify the condensate level (height above the tank bottom). In comparisons with the results of Table 1 it was assumed to be the same in all tests (0.21 m), which corresponded to the maximum value in two tests out of thirteen reported by *Dolgikh and Okunev* [*1989*], and the total height of the condensate above the evaporator was assumed to be 2.71 m (2.5 m from the tank bottom to the tube plus 0.21 m). ΔP was negative in all tests except 3 (Table 2), i.e. unidirectional fluid flow failed as in the previous tests.

Pazderin and Gilev [*2011*] repeated the experiment at the same conditions, for the tube lengths 200, 260 and 460 m, and monitored circulation by gauges of fluid level, pressure, and flow at the condenser inlet. The results of eight tests showed the condensate temperature to be warmer than the evaporator in three cases and ΔP to be negative in three other cases and positive in two tests [*Pazderin and Gilev, 2011*]. Thus, the cooling system obviously did not work, though the flow gauges showed ongoing circulation. Therefore, circulation in such systems with complex behavior should be monitored through transparent test section windows in tubes, which are commonly used to visually observe fluid patterns [*Pioro et al., 1991*]. Otherwise, responses of local loop fluid motion can be mistaken for normal circulation. Note that it remains unclear whether the system had achieved steady operation, as the experiment duration was not specified in the cited publications.

Thus, the available experimental data are insufficient to judge about the efficiency of such thermosyphons and to predict their cooling effect. With a laboratory model, it is easy to check whether condition (1) fulfills and, correspondingly, whether the system works or not (see below).

The operation of cooling systems was also studied theoretically [*Anikin and Spasennikova, 2014*] for large scope of working fluids, using the equation for flow of a liquid condensate within the segment ABCD (Fig. 2). With regard to (1) and (2) the flow becomes

$$KJ = P(t_c) + \rho g H_c - P(t_b), \tag{3}$$

where J is the liquid flow and K is the hydraulic resistance in the down-going part of the circulation path. The flow J can be positive (at sustainable operation), zero, or negative (when operation stops) depending on the sign in the right-hand side of (3). With the pressure at the condensate boiling point expanded along t_c as

$$P(t_b) = P(t_c) + \left(\frac{dP}{dt}\right)_{t_c} (t_b - t_c), \tag{4}$$

and the left-hand side in (3) denoted as Δp (pressure gradient required to overcome friction) [*Anikin and Spasennikova, 2014*], the equation is

$$\Delta p = \rho g H_c - \left(\frac{dP}{dt}\right)_{t_c} (t_b - t_c). \tag{5}$$

Note that transition from exact equation (3) to (5) already contains approximation in the form of (4) which can deviate strongly from the true value by nonlinearity of the $P(t)$ function and large $t_b - t_c$ difference. Furthermore, H_c is mis-interpreted as the height of the condenser (which part of it?) above the evaporator, but it cannot affect the fluid dynamics because the respective equation includes the evaporator level only. The expansion point $P(t_b)$ in (4) is assumed to be −20 °C though it would rather be equal to t_a, which differs from t_c for no more than a few degrees.

Then *Anikin and Spasennikova* [*2014*] infer that Δp is vanishing relative to the first term in the right-hand side of (5) and assume it to be zero. Taking into account the natural temperature constraints ($t_a < t_c$ and $t_b < t_m$) and the respective relationships for pressures ($P(t)$ growing monotonically)

$$P(t_a) < P(t_c),\ P(t_b) < P(t_m), \tag{6}$$

they arrive at a criterion implying that the system operates at (the right-hand side is positive)

$$H_c \le -\frac{t_a}{\rho g}\left(\frac{dP}{dt}\right)_{t_c}. \tag{7}$$

In (6) and (7), t_a is the air temperature ($t_a < 0$ °C in winter); t_m is the soil temperature (host medium for evaporator, assumed in that case to be $t_m = 0$ °C [*Anikin and Spasennikova, 2014*]).

The suggested criterion (7) contradicts the actual operation conditions, because it fulfills easier at a lower condensate level, but it has no relation with the amount of coolant charged into the thermosyphon: any minor amount (say, a few drops) of any fluid appears to be enough to satisfy the condition. However, the thermosyphon will obviously have zero efficiency in this case. Neglecting Δp in (5) on the basis of comparison with the first term only [*Anikin and Spasennikova, 2014*] is not a good approach. Instead, it should rather be compared with the sum of all terms (positive or negative) in the right side of (5). Furthermore, H_c, as well as t_c and t_b, are not constant but actually depend on t_a and t_m, system design, heat transfer, and hydraulic resistance.

A criterion similar to (7) follows from the exact equation (3) which, with regard to (6), leads to

$$KJ \ge P(t_a) + \rho g H_c - P(t_m). \tag{8}$$

Additionally, one of two conditions should fulfill: those of normal ($J > 0$) and blocked ($J \le 0$) operation. Only the latter condition is obviously consistent with (8). Correspondingly, the condition at which the system fails is

$$H_c \le \frac{P(t_m) - P(t_a)}{\rho g}. \tag{9}$$

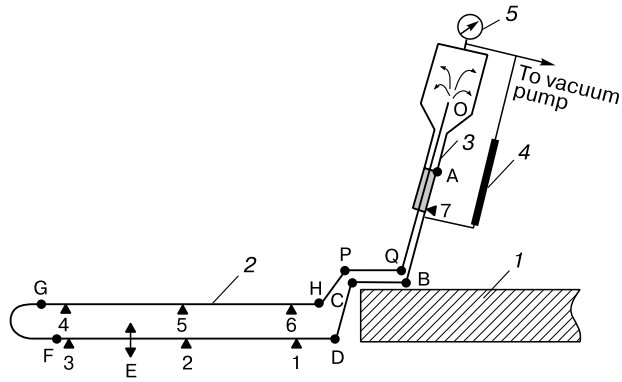

Fig. 2. Laboratory model of a thermosyphon with a horizontal evaporator.

1 – floor of cooling chamber; *2* – evaporator tube; *3* – condenser; *4* – tube for measuring condensate level; *5* – vacuum gauge. Bold triangles with numerals are thermistors. ABCDE is down-going condensate path; EFGHPQO is up-going path of two-phase flow; E – fluid boiling point.

Assuming $t_m = 0$ °C, with the pressure in the right-hand side expressed via the temperature gradient according to (4), one again arrives at (7), but it has a meaning of failure condition. It is better to use (9) for this purpose, with special caution, however, as H_c is not constant (see above). On the other hand, (1) includes empirical parameters and is undoubted, like the respective expression of the opposite sign corresponding to failure. Therefore, the results of the cited publications need revision.

LABORATORY THERMOSYPHON MODEL

The operation of thermosyphon cooling systems was tested using laboratory models as continuation of studies reported by *Gorelik and Gorelik* [*2011*]. It was noted earlier that the system was hard to start and unstable in operation. Namely, all condensate accumulated in the tank and did not sink into the evaporator, where the temperature and the saturation vapor pressure were higher than in the condenser, i.e., the system failed for some (not very clear) reasons.

Some new results were obtained with a laboratory model which was similar to that of *Gorelik and Gorelik* [*2011*] (Fig. 2) but had fully transparent glass tubes making visible all details of flow behavior instead of copper tubes with few windows. The evaporator was 13.7 m long and consisted of several serially connected tubes (about 1.15 m each) with an inner diameter of 10 mm and a wall thickness of 1 mm. The evaporator length being limited by the room size, the small tube diameter was selected to keep the length/diameter ratio the closest possible to that in the field. The pressure gradient inside the evaporator depended also on the coolant surface tension (depending, in

turn, on temperature). The evaporator-condenser temperature difference was about 30 °C; the respective pressure difference according to the saturation curve (for acetone) was of the order of 10^4 Pa, or three to four orders of magnitude (depending on temperature) higher than that under capillary forces, for the selected tube diameter. Smaller (mm-scale) tubes can be used as well, as in some tests of *Gorelik and Gorelik* [*2011*], but the circulation would be more difficult to observe. The length/diameter ratio in the laboratory model (with 10 mm diameter) approached 1500 and was about ten times lower than in the field. At higher ratios (e.g., 2500), the start and operation become more problematic [*Gorelik and Gorelik, 2011*].

According to the previous studies, fluid circulation became blocked in the end of the tube near the condenser inlet (HPQ in Fig. 2), where condensate pooled in an uncontrollable way. In order to reduce or remove the effect, that tube part was made larger: 20 mm diameter, the largest possible for the given configuration, only 1.6 times smaller than in the full-size system.

The evaporator tubes were laid on the concrete floor of the laboratory room, on wooden pads spaced at 1 m, to provide precise leveling of tube segments, in the absence of kinks in the connecting sleeves, and avoid influence of even minor (1–2 cm) vertical or horizontal shifts on the start and operation. Note that, in the field conditions, evaporators made as flexible plastic tubes hundreds of meters long are laid on a pad prepared normally during ground leveling, and are buried under soil fill (the structure foundation) compacted by operating machinery and the structure loads. The tubes are inevitably subject to vertical and horizontal deformations (though this effect has never been discussed in the literature), which are natural and cannot impede sustainable operation of thermosyphons. Numerous laboratory tests demonstrate that the system behavior is insensitive to vertical or horizontal shifts of tube segments. The blockage is restricted to the HPQ segment (Fig. 2).

The experiment was run with the same method as in [*Gorelik and Gorelik, 2011*], using an acetone

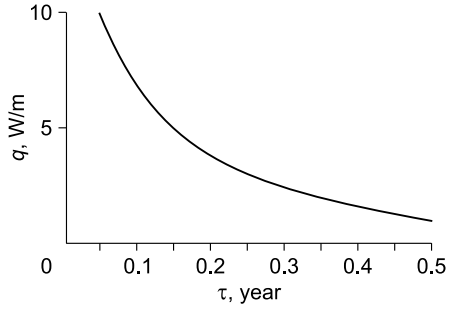

Fig. 3. Time-dependent (τ) heat flux (*q*) variations on evaporator wall.

coolant. Unlike many other industrially used fluids, acetone has the saturation vapor pressure below the atmospheric pressure for a large range of positive temperatures, which ensures cheap, straightforward, and safe handling of the model. The chemistry of the working fluid does not interfere with the basic fluid dynamic principles and system operation, but affects only the magnitudes of parameters [*Pioro et al., 1991*].

THERMAL LOADS

It is pertinent to compare laboratory and field systems in terms of heat flux to evaporators. At a constant temperature of the evaporator wall t_s and the initial ground temperature t_0, heat flow $q(\tau)$ per unit length of a tube in an infinite space is [*Carslow and Jaeger, 1959*]:

$$q(\tau) = \frac{8\lambda_f\left(t_0 - t_s\right)}{\pi} \times \\ \times \int_0^\infty \exp\left(-\phi(\tau)z^2\right)\frac{dz}{z\left(J_0^2(z) + Y_0^2(z)\right)}; \quad (10)$$

$$\varphi(\tau) = \frac{\kappa_f n\tau}{a^2}. \quad (11)$$

were λ_f and κ_f are, respectively, the thermal conductivity and diffusivity of frozen soil; a is the tube radius; n and τ, respectively, are the number of seconds in a year and the time (years) since the start of cooling; J_0 and Y_0 are the Bessel functions.

Generally speaking, t_s depends in a complex way on climate and thermosyphon design, but due regard for this dependence in engineering calculations is impossible at the time being. The common practice is to use winter means of climate parameters and some models of design and fluid dynamics in thermosyphons. Assuming that soil is cooled at a constant winter mean air temperature t_a, the evaporator walls cannot be colder than air (t_s is never lower than t_a), while the thermal loads cannot exceed those according to (10) and (11) at $t_s = t_a$. The theoretically possible minimum heat flux for a given climate can be estimated (Fig. 3) assuming $t_a = -13$ °C typical of the northern Tyumen region; $t_0 = -0.1$ °C, $a = 0.016$ m, $\lambda_f = 1.8$ W/(m·°C), and $\kappa_f = 8\cdot10^{-7}$ m^2/s. Except for the first winter month, heat flux is within 7 W/m, which is below the least possible thermal load produced by heaters in the experiments of *Dolgikh and Okunev* [*1989*]. Actually, t_s is much higher than t_a due to the effect of hydraulic and heat losses in the system. Approximate modeling [*Gorelik, 1980*] based on the concept of thermal effect radius [*Barenblatt, 1954*] shows that t_s never falls below −10 °C (in our case), i.e., the thermal load never exceeds 5 W/m, at the most favorable choice of the initial parameters.

The laboratory evaporator is a glass tube of an inner diameter of 10 mm and a wall thickness 1 mm, and its heat exchange with room air occurs by natural convection. The heat flow per tube unit length, estimated with reference to the handbook of *Wong* [*1977*], at the observed 15–20 °C temperature gradient between the evaporator wall and the air (at normal operation), is 3–5 W/m, which agrees with the estimated field thermal loads.

RESULTS OF LABORATORY TESTS

The HET thermosyphon system is designed assuming that both phases of the working fluid move in same direction along the tube, between the condenser outlet and inlet, while the flow structure changes continuously according to the vapor percentage. However, *Gorelik and Gorelik* [*2011*] reported a continuous counter flow of condensate against the up-going two-phase flow within the segment HPQ (Fig. 2). The flow structure was observed visually along the whole tube length since the start of the system (cooling chamber). Before the start, all condensate remained accumulated within the horizontal part of the evaporator near the condenser outlet. After the start, the air cooled down and the saturation vapor pressure decreased, which caused both down- and up-going flows of the coolant (mainly the vapor phase) into the condenser. Vapor condensed on the condenser walls and flew into its narrow bottom part. The growing liquid level in it impeded the down-going vapor flow, which in a while became restricted to the up-going segment FGHPQO.

As the temperature in the cooling chamber fell to –4 or –5 °C (at 20–25 °C in the room), the pressure dropped markedly, both in the condenser and in the evaporator. When the evaporator heated up, the fluid in it began to boil, most easily at the point E located near the end of the liquid flow, where resistance to external pressure was the lowest. Since that time on, while the condenser was being further cooled (till the technologically feasible temperature –13.5 °C), the liquid flow was seen clearly. It was rather uniform all along the tube (down the flow after E), but its rate changed slightly with time. That was the flow of a condensate plug detached from the main condensate body at E, which moved at 1 to 3 m/s depending on the condenser cooling at normal operation. Sometimes there were two concurrently moving plugs, quite far apart. They were 5–10 cm long and slightly shorter between E and gauge 5, due to liquid evaporation, and slightly longer between gauge 5 and the cooling chamber, due to return flow involved into the condensate at QPH and down the flow.

It is the inevitably arising return flow of condensate that differs the real fluid behavior from the theoretical idea of unidirectional flow. It means that the two phases move in opposite directions within a segment of a finite length. The counter flow exists since the onset of liquid circulation and is observed in the tube from outside of the cooling chamber, both at normal (Fig. 4, *a*) and blocked (Fig. 4, *b*) operation. This fact is of key importance as the two-phase systems with counter flow are known to develop a slug and plug regime that leads to failure [*Wallis, 1969; Bezrodnyi, 1978; Kharitonov and Shirikhin, 1991*]. This regime and its predictions for different configurations were largely discussed in the literature [e.g., *Taitel and Dukler, 1976; Vasiliev et al., 1978; Pioro, 1982; Vasilieva and Kosmacheva, 1987*], but no universally accepted general approach has been suggested.

At normal operation, the flow between P and Q is either stratified (with up-going vapor counter flow and down-going return flow of liquid, as in Fig. 4, *c*), or turbulent with a vapor-liquid flow over the down-going liquid flow in the tube bottom (Fig. 4, *d*). The circulation becomes blocked when a stable condensate plug occupies the whole tube section between P and Q (Fig. 4, *e*).

The blockage often occurs early during operation: a return flow forms within the PQO segment 10 to 15 min after the onset of liquid circulation and continues in the lower part of the fluid (from H to P and downflow). The return flow grows progressively as the condenser cools down while the counter vapor-liquid flow remains almost stable. At some point, the return flow becomes as large as to occupy the whole tube section within PQ and forms a plug. The plug blocks the up-going flow, which fails to overcome the plug resistance, possibly, because the stored energy is too low at small thermal load on the evaporator. The flow inside the plug is restricted to slow motion of a few vapor bubbles toward the condenser (Fig. 4, *e*). The plug is stable and persists even on strong shaking. On the other hand, it shows dynamic behavior as some liquid sinks into the evaporator even during blockage (Fig. 4, *b*), though the plug length remains invariable. Thus, there may be local loops in fluid circulation near the evaporator terminals: the condensate sinks into the evaporator where it evaporates, then flows back and condenses within the cold segment of the return flow (inside the chamber). While the circulation is blocked, the evaporator quite rapidly reaches the room temperature, and the pressure in it increases to become sufficient for forcing all liquid down into the condenser. All condensate accumulates in the condenser and stays there (apparently, likewise forming a circulation loop), while only traces of liquid are observed in the evaporator. The condensate level in this case is about 30 cm (Fig. 4, *f*), whereas it does not exceed a few cm at normal operation.

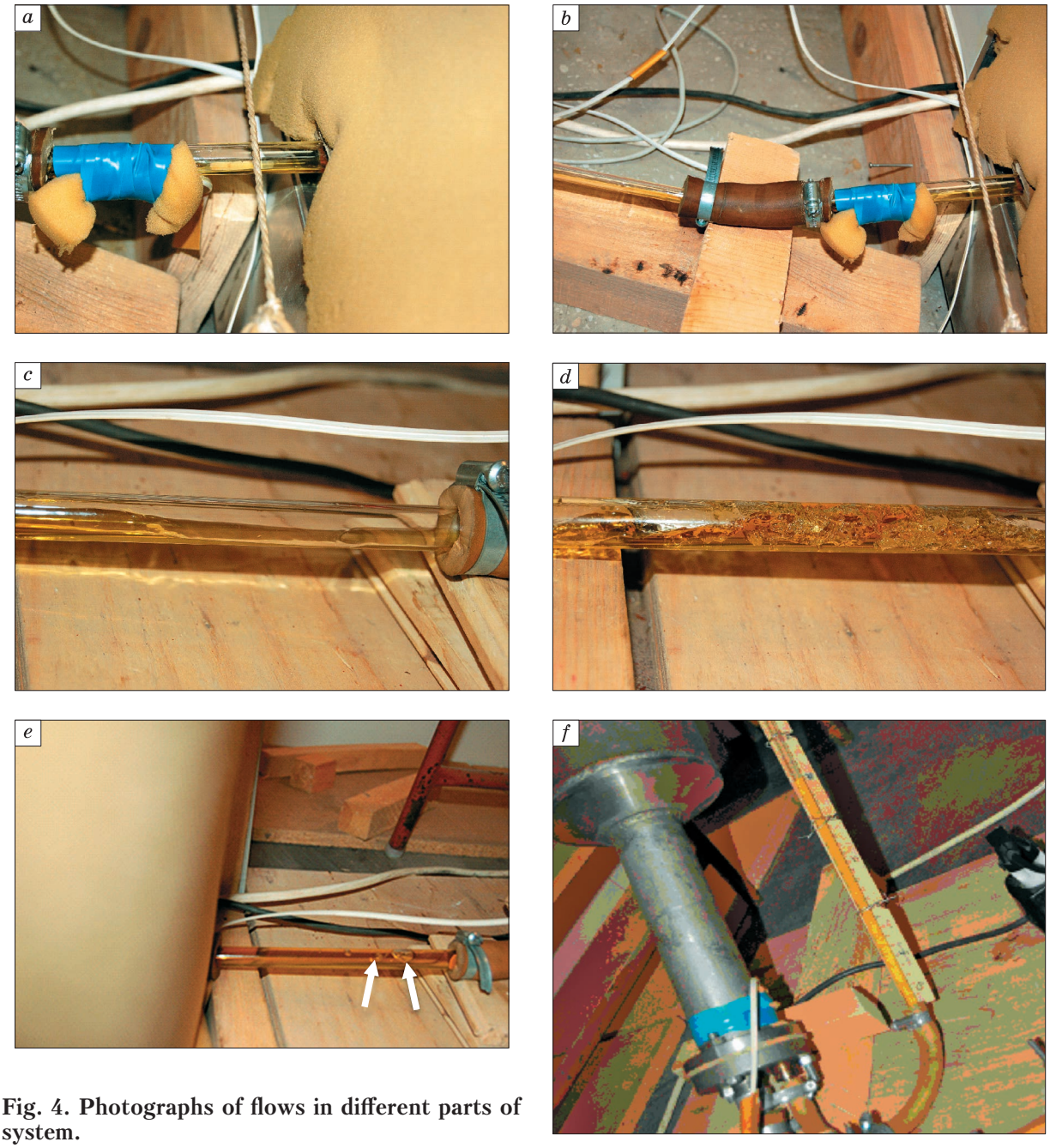

Fig. 4. Photographs of flows in different parts of system.

a – sinking condensate before inlet into cooling chamber (segment HP), normal circulation; *b* – sinking condensate in segment HP, blocked circulation; *c* – laminar flow within segment PQ (inside cooling chamber), normal circulation; *d* – turbulent flow within segment PQ, normal circulation; *e* – condensate plug within segment PQ, blocked circulation (arrows show vapor bubbles); *f* – condensate level, blocked circulation (see a condensate level measuring tube with a scale on the right).

Note also that the validity of (1) is easy to check in laboratory: $\Delta P < 0$ if the system does not work, at $H_c = 0.40$ m according to temperature and vacuum gauge readings (Fig. 5, *a*), and at the greatest condensate level, with regard to the floor height (Fig. 4, *f*); if the system operates normally, $\Delta P > 0$ is inferred from curves of Fig. 5, *b*, *c* and the condensate level. One should bear in mind that the vacuum readings measure excess pressure, which is negative for acetone saturation vapor. The pressure magnitude used in (1) corresponds to the measured value plus 1 bar.

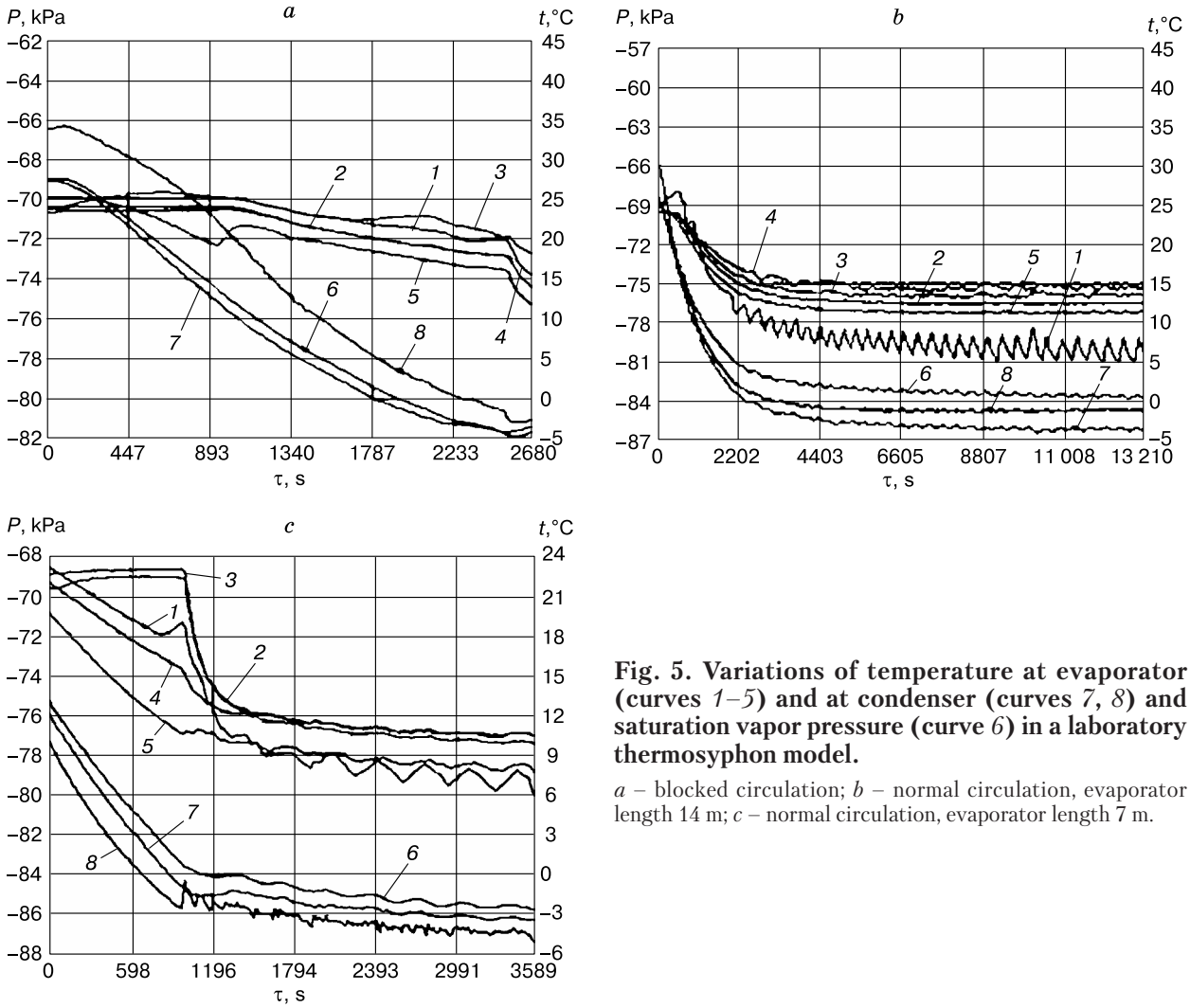

Fig. 5. Variations of temperature at evaporator (curves *1–5*) and at condenser (curves *7*, *8*) and saturation vapor pressure (curve *6*) in a laboratory thermosyphon model.

a – blocked circulation; *b* – normal circulation, evaporator length 14 m; *c* – normal circulation, evaporator length 7 m.

IMPROVING SYSTEM SUSTAINABILITY

When the thermosyphon operates normally, the evaporator cools down quite rapidly to a steady temperature depending on the tube length (Fig. 5, *a*, *b*). In this case, fluid circulation is sustainable for several hours without slug and plug. If the condenser is relatively cold, the system can be started by special measures (that ensure sustainable fluid circulation) designed during laboratory testing of the model. To improve the efficiency and sustainability of thermosyphon operation, an electronic unit of start control is incorporated into the system configuration. The control unit includes electromagnetic sensors that measure the parameters of the system and the environment; an analyzer of readings and an on/off (open/close) electromagnetic valve triggered by an electric signal which the analyzer generates based on a criterion saved in its memory. The valve is set into the evaporator tube slightly below the plug segment (below H in Fig. 2). Thermistors placed on the condenser and evaporator outer walls can monitor the environment, while the temperature, pressure, or condensate level measurements are used to monitor the state of the system.

The valve can close or open, for example, at a certain condensate level. At normal operation, it has the minimum height (h_{min}) above the evaporator (taken for a base level), found empirically or through calculations. In the slug and plug regime, all condensate accumulates in the condenser, and its level is the highest h_{max}, which is easy to estimate knowing the condenser specifications and the amount of charged working fluid. In the warm season, when air is warmer than the ground to be cooled by the thermosyphon, the latter is in its pre-start state, with all condensate in the tube, at the lowest possible height. The condensate level gauge shows a value below h_{min}, and the

condition $h < h_{min}$ is saved in the analyzer's memory as a criterion for generating the signal that closes the valve.

In the cold season, air cools down, and the temperature inside the condenser falls correspondingly, leading to the respective decrease in the saturation vapor pressure. When the evaporator temperature and the respective vapor pressure remain constant while the air becomes cold enough, the pressure gradient arising between the evaporator and the condenser induces flow of liquid from the evaporator to the condenser along FDCBA (while the valve is closed), and soon all liquid becomes accumulated there. The condenser design prevents condensate leakage into the zone above the valve (above H in Fig. 2), and no plug can form.

According to the field experience, valve opening at $h > 0.8h_{max}$ can provide sustainable circulation and efficient operation of thermosyphons. This start condition is reliable and stable because the up-going evaporator path GHPQO has minimum hydraulic resistance and maximum flow kinetic energy at the time when the valve opens, which precludes the slug and plug regime (typical of low-energy two-phase flow). Thus the condition $h > 0.8h_{max}$ is acceptable as a criterion for the signal to open the valve. If air temperatures during the cold season casually wave to above the current ground temperature, the condensate sinks into the evaporator, and the valve closes according to the $h < h_{min}$ criterion; as the air cools down again, the $h > 0.8h_{max}$ criterion triggers valve opening. Thus, the automatic start controlled by the condensate level ensures sustainable system operation.

In the same way, the system can be started according to condenser or evaporator temperatures. At normal operation, the condenser temperature is the highest and that of the evaporator is the lowest (both found by calculations or empirically for the given air temperature); when circulation is blocked, the condenser is the coldest, about the ambient air temperature, and the evaporator is the warmest, about the ground temperature. The criteria for the control signal that closes or opens the valve are selected empirically. The system can be likewise started according to condenser or evaporator pressures, which are proportional to temperatures in the saturation curve. For better stability, synchronous readings of different gauges can be used. Such a method for improving the sustainability of thermosyphons has been patented [*Melnikov et al., 2015*], but it may be prone to failure in the filed.

CONCLUSIONS

Laboratory testing of a two-phase thermosyphon with a horizontal evaporator, classified as a direct-flow system, reveals the existence of a counter-flow segment in the fluid circulation path at evaporator thermal loads within 5–7 W/m, about those in soil. Liquid in this segment moves against the two-phase flow and sinks into the evaporator, which contradicts the ideal design of unidirectional fluid flow all along the circulation path (at least for small thermal loads). Thus, the process turns to the slug and plug regime when the condensate blocks the flow into the condenser, and the system fails.

The operation sustainability of thermosyphons can be improved using a close/open valve, which is set into the evaporator tube below the counter-flow segment and is triggered automatically as the condenser cools down and the system reaches certain empirically constrained values of parameters (e.g., condensate level, temperature, or pressure).

The method has demonstrated high efficiency in laboratory but its field application may be problematic because electronic units are vulnerable to open-air effects. Therefore, further research is required to find the appropriate solution.

The study was supported by grant SS-3929.2014.5 for leading science schools from the President of the Russian Federation and was carried out as part of Basic Research Program 12 of the Geosciences Department of the Russian Academy of Sciences.

References

Anikin, G.V., Spasennikova, K.A., 2014. About choice of refrigerating fluid for the seasonal cooling devices of "HET" type. Earth Cryosphere (Kriosfera Zemli) XVIII (2), 31–33.

Barenblatt, G.I., 1954. Some approximate methods in the theory of 1D unsteady fluid filtration in elastic conditions. Izv. AN SSSR. Ser. Teckhn. Nauk, No. 9, 35–49.

Bezrodnyi, M.K., 1978. The upper bound of heat transfer in evaporating thermosyphons. Teploenergetika, No. 8, 63–66.

Carslow, H., Jaeger, J., 1959. Conduction of Heat in Solids. Oxford University Press, London, 487 pp.

Dolgikh, G.M., Dolgikh, D.G., Okunev, S.N., 2004. Freezing of soils: Engineering solutions of *Fundamentstroiarkos* Company, in: The Cryosphere of Petroleum Provinces. Proc. Intern. Conf., Tyumen, pp. 56.

Dolgikh, G.M., Okunev, S.N., 1989. Conservation Measures and Environmentally Safe Technologies for Development of Gas and Condensate Fields in the Yamal Peninsula. Giprotyumenneftegaz, Tyumen, 152 pp. (in Russian)

Dolgikh, G.M., Okunev, S.N., 2006. Construction and stabilization of cooled foundations in permafrost by *Fundamentstroiarkos* Company: Promising engineering solutions, in: Theory and Practice of Permafrost Assessment and Predictions. Proc. Intern. Conf., Tyumen, Book 2, pp. 228–232.

Dolgikh, G.M., Okunev, S.N., Strizhkov, S.N., Pazderin, D.S., Gilev, N.G., 2011. Operation of thermosyphons, from data of pilot tests, in: Permafrost Engineering. Proc. Intern. Conf., Tyumen, 7–10 November, 2011, Tyumen, pp. 36–42.

Feklistov, V.N., Dolgikh, G.M., Okunev, S.N., Pazderin, D.S., 2008. Investigation into HET thermosyphons for soil stabilization, in: Resources of Polar and Highland Areas. State and Prospects of Geocryology. Proc. Intern. Conf. Book 2, Tyumen, pp. 165–168.

Gorelik, J.B., 1980. Modeling soil temperature field around vapor-liquid thermopiles. Probl. Nefti i Gaza Tyumeni, Issue 47, 58–61.

Gorelik, J.B., 2012. Laboratory study of the devices for termostabilization of frozen ground, in: Proc. 10th Intern. Conf. on Permafrost (TICOP), Pechatnik, Salekhard, pp. 10.

Gorelik, J.B., Gorelik, R.J., 2011. Laboratory research of work of the natural convectional biphase cooling device with horizontal evaporative part. Kriosfera Zemli XV (2), 34–43.

Kharitonov, A.N., Shirikhin, Yu.N., 1991. Crisis of heat transfer in low-angle inclined evaporators of two-phase thermosyphons. Prom. Teplotekhnika 13 (1), 77–83.

Kutepov, A.M., Sterman, A.S., Styushin, A.G., 1986. Fluid dynamics and heat transfer on evaporation. Vysshaya Shkola, Moscow, 448 pp. (in Russian)

Lyakh, A.A., Maltsev, V.V., Osadchii, G.S., Shirikhin, Yu.N., 1978. Cooling concrete masses by thermosyphons: Field testing, in: Improving Efficiency of Thermal Treatment of Reinforced Concrete. Proc. All-Russian Conf. Kiev, pp. 15–16.

Melnikov, V.P., Gorelik, J.B., Nakladnov, V.V., 2015. A Direct-flow Thermosyphon for Stabilization of Permafrost. Patent 2554955 Russian Federation, MPK E02D 3/115(2006.01)/ Priority 31.03.14; Publ. 10.07.15, Bull. 19.

Pazderin, D.S., Gilev, N.G., 2011. Field experimental testing of HET-460 thermosyphons, in: Strategy of Innovation Development in Extreme North. Proc. All-Russian Conf., Tyumen, pp. 255–263.

Pioro, I.L., 1982. Limit heat transfer parameters in two-phase thermosyphons. Prom. Teplotekhnika 4 (4), 25–30.

Pioro, I.L., Antonenko, V.A., Pioro, L.S., 1991. Efficient heat transfer systems with two-phase thermosyphons. Naukova Dumka, Kiev, 246 pp. (in Russian)

Taitel, Y., Dukler, A.E., 1976. A model for predicting flow regime transition in horizontal gas-liquid flow. AICE J. 22, 47–55.

Vasiliev, L.L., Grakovich, L.P., Khrustalev, D.K., 1978. Limit parameters of inclined thermosyphons and heat tubes with excess working fluid. Inzh. Fiz. Zhurn. 16 (5), 709–716.

Vasilieva, G.V., Kosmacheva, E.M., 1987. Boiling crisis in thermosyphons. Nauchnye i Prikladnye Problemy Energetiki: Nauch. Tekhn. Sb., No. 14, 58–62.

Velchev, S.P., Sizikov, L.V., 2008. Soil cooling for thermal stabilization of permafrost under tanks, in: Resources of Polar and Highland Areas. State and Prospects of Geocryology. Proc. Intern. Conf. Book 2, Tyumen, pp. 67–69.

Wallis, G., 1969. One Dimensional Two-Phase Flow. McGraw-Hill, New York, 440 pp.

Wong, H.Y., 1977. Handbook of Essential Formulae and Data on Heat Transfer for Engineers. Longman, London, New York, 236 pp.

Received March 3, 2015